

Development of a Vanadium Redox Flow Battery for Energy Storage

Gianluca Ghirlanda
gianluca.ghirlanda@tecnico.ulisboa.pt

Instituto Superior Técnico, Universidade de Lisboa, Portugal

November 2018

Abstract

Vanadium Redox Flow battery (VRFB) is an electrochemical energy storage system which presents a high potential in terms of grid-scale renewable energies storage solution. A fundamental and inexpensive design for a lab-scale VRFB is presented in this work, along with the basic step for the electrolyte chemical preparation from V_2O_5 . The electrochemical cell has 25 cm^2 of area without any specific flow path geometry and it is assembled using raw material of easy availability and tested with different working conditions and performing acid treatment on the electrodes. It has been tested with two different concentration of active species, 0.15 M and 0.3 M of vanadium. Polarization curves, charge-discharge cycles, self-discharge curves and electrochemical impedance spectroscopy are used as tools to investigate the influence of the different working conditions and treatment on the efficiency of the electrochemical cell. The space-time test was also performed to understand the mass transport behaviour inside the cell. The outcomes from EIS exhibit an improvement with an increment of the concentration and it shows the membrane has a purely resistive behavior. Among the different conditions tested in this work, better performance were achieved using the acid treated electrode and the more concentrated electrolytes, which presented current density of 40 mA/cm^2 . The cell presented an improvement in charge-discharge cycles as well as in the polarization curves and self-discharge curves.

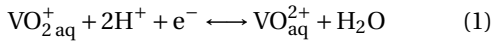
Keywords: Vanadium Redox Flow Battery, Electrochemical Energy Storage System

1. Introduction

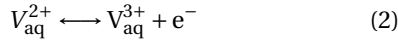
The efficiency and the fast response of the energy storage system (ESS) are important assessment parameters as well as the lifetime and the investment and operational costs. The redox flow batteries are one of the most promising technologies: they combine good efficiency, short response time, reliability and long lifetime. The energy conversion is based upon the reversible electrochemical reactions of two redox couples and they are normally dissolved in the electrolyte solutions. Unlike conventional batteries where the redox-active materials are confined inside the electrodes, the redox flow batteries sometimes referred as reversible fuel-cells, store energy in electrolytes that are pumped into the battery stack for energy conversion. This working mechanism avoids the electrodes from undergoing structural changes, complex redox reactions and mechanical strains, increasing their working life [1]. The main characteristic of these energy storage systems is the total autonomy between the installed power and the stored energy, making the technology very versatile depending on the necessities and the application field [2]. Several redox-active materials were utilized for redox flow batteries. In recent years the unique concept and mech-

anism of redox flow battery technology, namely the flowing of redox-active material and the extendable energy capacity, have attracted a great interest in research and development. The redox flow batteries are electrochemical devices able to convert chemical energy from electrolytes into electrical energy and vice versa, through a redox reaction. For this reason the electrolytes are essential components of the battery. They are stored inside tanks and they flow into the cell driven by a pump inside the half-cells where the reactions take place and the charge is transferred. The released electrons flow into an external electric circuit and they determine the continuous current supplied or absorbed from the battery. The two electrolyte are always separated from each other, due to the presence of the proton exchange membrane. It allows the proton transfer from one half-cell to the other and it blocks the mix of the two solutions. The decision is to focus the attention on the vanadium redox flow battery because this type of redox flow battery suppresses the issue of irreversible cross contamination, using only one redox-active species which is characterized by four oxidation states. One disadvantage of Vanadium redox flow batteries is the small volumetric energy storage capacity, limited by the low solu-

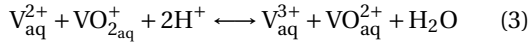
bility of the active species in the electrolyte [3]. The cost of vanadium is acceptable because it is a relatively abundant material, which exists naturally in 65 different minerals and fossil fuel deposits. However, the system requires the using of expensive ion-exchange membrane, which can contribute more than 40% of the overall battery cost [4]. To overcome these limitations and promote the development of the performance, there are two main approaches: on one hand to focus the attention on the basic physical phenomena behind its operation, on the other hand develop specific components designed to satisfy the precise needs of redox flow batteries. The redox reaction involves the four different vanadium oxidation state, at which correspond different colors.
Cathodic reaction:



Anodic reaction:



The overall reaction is:



From left to right in discharge mode while in the opposite sense is charging mode.

2. Methodology

2.1. Cell potential and State of Charge (SOC)

The cell potential is the sum of the interfacial potentials of the cathode and the anode and Nernst equation gives a relationship between the equilibrium potential of the electrode, the concentration of the reagent and products. When the total vanadium ions concentrations are the same for both electrolytes, the the state-of-charge (SOC) in relation with the vanadium ion concentrations is given by [5]:

$$\text{SOC} = \left(\frac{c_{\text{V}^{2+}}}{c_{\text{V}^{2+}} + c_{\text{V}^{3+}}} \right) = \left(\frac{c_{\text{VO}_2^{+}}}{c_{\text{VO}_2^{+}} + c_{\text{VO}^{2+}}} \right) \quad (4)$$

Therefore, it is possible to deduce the state of charge during the cell operation only measuring the open circuit potential. Despite the measure is not accurate, it is widely used as first approximation because of its rapidity. The OCP can be expressed in terms of the SOC:

$$\begin{aligned} E_{\text{cell}} &= E_{\text{cell}}^o - \frac{RT}{nF} \ln \left(\frac{c_{\text{V}^{3+}} c_{\text{VO}^{2+}}}{c_{\text{V}^{2+}} c_{\text{VO}_2^{+}} c_{\text{H}^{+}}^2} \right) \\ &= E_{\text{cell}}^o - \frac{RT}{nF} \ln \left(\frac{(1 - \text{SOC})^2}{\text{SOC}^2 \cdot c_{\text{H}^{+}}^2} \right) \end{aligned} \quad (5)$$

2.2. Current, potential and energy efficiency

The performance of a battery is evaluated through its efficiency. The current efficiency is [6]:

$$\eta_i = \frac{Q_d}{Q_{\text{ch}}} = \frac{\int_{t_{\text{ch}}}^{t_d} i_d dt}{\int_0^{t_{\text{ch}}} i_{\text{ch}} dt} \quad (6)$$

It describes the electron transfer performance and it takes into account the side reactions and the crossover, that is the reduction of the battery's capacity and the imbalance of the solution due to the active species crossing through the membrane.

The potential efficiency is [7]:

$$\eta_E = \frac{\bar{E}_d}{\bar{E}_{\text{ch}}} = \frac{\int_{t_{\text{ch}}}^{t_d} E_d dt}{\int_0^{t_{\text{ch}}} E_{\text{ch}} dt} \quad (7)$$

This parameter takes into account the losses due to the overpotentials. Despite the current efficiency, it decreases when the current density increases because it intensifies the ohmic losses.

The energy efficiency describes the overall performance of the battery [6]:

$$\eta_{\text{en}} = \eta_i \eta_E = \frac{\int_{t_{\text{ch}}}^{t_d} E_d i_d dt}{\int_0^{t_{\text{ch}}} E_{\text{ch}} i_{\text{ch}} dt} = \frac{\int_{t_{\text{ch}}}^{t_d} P_d dt}{\int_0^{t_{\text{ch}}} P_{\text{ch}} dt} \quad (8)$$

To optimize the performance of the battery is necessary to consider the effect of each intervention in both efficiency parameters and to not neglect any undesired phenomena during the operation of the battery.

3. Experimental

The objective of the work is to optimize a lab scale VRFB and study its performance in different working conditions.

3.1. Equipment

The system comprises a single cell. The cell active area is 25 cm² and the electrodes are Carbon Felt grade VGD NATIONAL™ (Ohio, US) 10 mm of thickness. The electrodes were first tested as brand new and H₂SO₄ treatment was carried out on the same type of electrodes and tested thereafter. The electrode were boiled in pure H₂SO₄ for 5 h and rinsed thoroughly. The current collectors are made of copper and a polymeric graphite plate is placed between the porous electrode and the current collector. NAFION®117 by Dupont™ (Delaware, US) is used as membrane to separate the anode and the cathode compartments and to allow the protons transfer. Prior to use, hydration of the membrane was made boiling it in 3% w/v H₂O₂ for 1 hour in order to remove all the impurities. Then it was slightly boiled in 1 M of H₂SO₄ for 2 hours at 80°C in order to increase the amount of protonated sulfonic acid groups to enhance the overall ionic exchange ability of the membrane. The electrolytes consist of 200 mL of 0.15 M of vanadium ions

in 3 M of H_2SO_4 obtained from V_2O_5 dissolution. In order to prevent the oxidation of the anolyte by atmospheric O_2 , nitrogen was supplied to the negative side continuously. More concentrated solutions of 0.3 M of vanadium and 6 M of H_2SO_4 was tested lately to understand the influence of the concentration on the electrochemical performance of the cell.

3.2. Marker experiment

The cell was filled continuously with the anolyte to one side and with H_2SO_4 on the other side at the lowest flow rate of 2.5 mL/min. The marker solution consisted on 10 mL of 3 M of H_2SO_4 with 0.15 M of V^{5+} ions. The space-time was measured injecting the marker solution into the side where H_2SO_4 was flowing and record the current response of the cell. When the marker was injected a peak in the current density plot as a function of time and a slow reduction due to the exit of the active species from the cell are evident as shown in Figure 1.

3.3. Polarization curves

The polarization curves are useful to analyze the generic loss of an electrochemical cell and if coupled with electrochemical impedance spectroscopy (EIS), they can give a specific interpretation of the limits on the performance of the battery [8]. The tests were performed during discharging from a potential less than the OCP until the limiting current due to mass transport effects was reached. The performance curves were recorded at different values of flow rate, namely 2.5 mL/min, 5 mL/min, 10 mL/min and 16 mL/min. The values of the flow rate were chosen according to the rotational velocity range of the peristaltic pump in order to obtain a uniform variation between each flow rate. The polarization curves were used as tool to assess the acid treatment performed in the electrodes. Then the next tests were performed with the most efficient electrode with electrolytes with double of the concentration.

3.4. Charge and Discharge cycles

The objective of the charge and discharge cycles test is to obtain information upon the efficiency of the battery. The volume of the electrolytes was limited just on the amount inside the cell and without the use of the pump. The tests cannot replace a more complete dynamic tests where the solution are circulating and there is a progressive decrease in the state of charge of the tanks. Nevertheless, these type of tests are enough to understand the performance of the battery in short times [9].

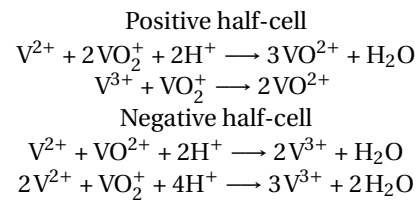
The solution were charged at constant current of 100 mA until the potential value of 1.7 V in order to avoid high overpotential that can cause side reaction such as hydrogen evolution in the $\text{V}^{2+}/\text{V}^{3+}$ compartment [10] and graphite corrosion in the $\text{VO}_2^+/\text{VO}^{2+}$ compartment [11]. The same current intensity value was

used during discharge.

The test were performed for the acid treated electrodes and the non-treated electrodes, and the electrolytes with the two different concentrations.

3.5. Self-discharge plots

The tests aim to evaluate the self-discharge for the electrolyte inside the cell and the permeability of the membrane to the active species that might cause self-discharge. The tests were performed without flow, to reproduce the real application of the battery during its rest time. In particular, the reactions induced by vanadium ions crossover are [12]:



Prior, charge was made galvanostatically at 100 mA for the time evaluated in the charge-discharge cycles and then the OCP was recorded in function of time. The test were performed for 0.15 M and 0.3 M of vanadium ions.

3.6. Electrochemical Impedance Spectroscopy (EIS)

The EIS records the response of the device to a sinusoidal signal of potential applied of fixed amplitude and decreasing frequency. The response of the system will be a current signal which will be characterized by a phase shift and damping. This allow to create an equivalent circuit which represent the internal resistance of the device at the different frequencies applied. The Nyquist diagram plots the impedance as imaginary and real part while Bode diagram as phase and frequency [13].

At each frequency different phenomena take place. At high frequencies the kinetic effects while at low frequencies the mass transport effects.

The range of small frequencies field was not studied in this work because of dispersion and to minimize the time evolution of the system. The EIS was run between the 100 kHz and 100 mHz with a step decay of 10. The signal was chosen by the potentiostat. The EIS was carried out with electrolytes flow at 16 mL/min for the different concentrations of vanadium in the electrolytes. The influence of the membrane in the internal resistance of the cell was evaluated, performing an EIS with two membranes in series.

4. Results

4.1. Marker experiment

The current and charge responses to the marker injection as function of time are shown in Figure 1.

The injection was done at 150 s after the current was stable for 1 minute. Although the geometry of the cell does not ensure the complete recirculation of the

marker due to possible stagnation points, it is assumed the space-time is reached when the current is stable for one minute at 15% of the current peak. The current peak corresponds to 0.07 A and the time for the current to stabilize at 0.03 A is around 550 s.

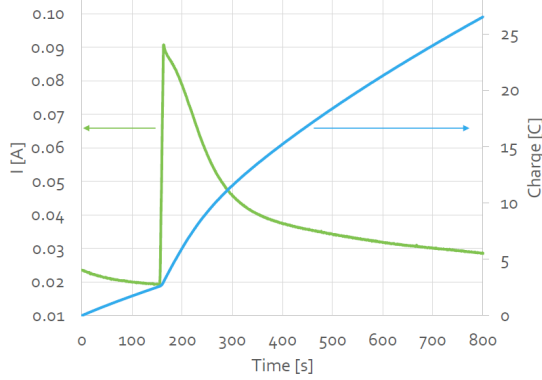


Figure 1: Current and charge response to the marker experiment

The space-time is dependent upon the geometry of the cell, so it will not change for the other half-cell, but the peak current might have changed if the other half-cell was tested. There is a high distribution of space-time yield proven by the high peak. The half of the species contained in the marker was converted in the first 100 s. The amount of active species injected corresponds to:

$$Q_{av} = VcF \quad (9)$$

The area below the current peak correspond to the amount of active species actually converted, in particular:

$$Q_{conv} = \int_{150}^{800} (i(t) - i_0) dt - \int_0^{150} i(t) dt \quad (10)$$

where i_0 is the value of the current before the injection, 20 mA. The conversion efficiency is defined as:

$$\eta_{conv} = \frac{Q_{conv}}{Q_{av}} = \frac{i A_e}{F c \dot{Q}} \quad (11)$$

and in this case it corresponds to 10%.

4.2. Flow rate influence on polarization behaviour

The effect of the scan rate on the polarization behaviour has been investigated in order to choose the scan rate at which perform the experiments. The longer measurement periods with lower scan rates resulted in higher contamination of the electrolyte causing a significant reduction in the active species and the electrolytes needed to be charged. In order to reduce the time in which the experiments were carried out and to not compromise too much the electrolytes with the LSV tests it was chosen to use a scan-rate of 10 mV/s.

The results show an linear increase in current density with an increase in the flow rate. There is a relevant increment between 2.5 mL/min and 5 mL/min and it is probably because of a more uniform distribution of the electrolyte inside the cell and the increase of the turbulence avoided stagnation points which may cause a decrease in current density. It is evident that at low flow rates both activation overpotential and the mass transport effect are relevant already at low current densities. It can be explained because the flow rate is not sufficiently strong to ensure the replacement of the solution absorbed by the electrode with new reagents that start to be insufficient, also because of the very deep weft of the carbon felt. The ohmic linear part shows an improvement with the increase of the flow rate, which lead to an increase of the power of the cell. The maximum amount of current density was 10 mA cm^{-2} at 16 mL min^{-1} . The range of maximum power supplied by the cell in these conditions are 7 mW cm^{-2} and 12 mW cm^{-2} .

4.3. Acid treatment influence on polarization behaviour

The influence of the flow rate was then investigated for the acid treated electrodes and then compared with the results obtained for the non-treated electrodes.

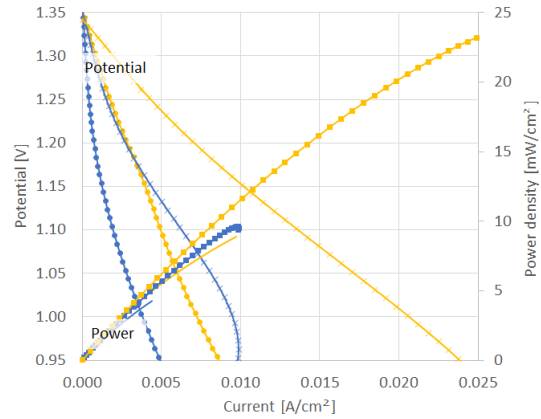


Figure 2: Polarization curves for 2.5 mL/min (blue), 16 mL/min (orange) for NT (circle) and AT (cross) and relative power NT (no marker) and AT (squares)

As shown in Figure 2 the acid treatment on the electrodes exhibits an overall increment in current density. The lower flow rate for both electrodes show a detachment from the lowest current densities, presenting an evident section due to activation losses. The influence of the flow rate in the electrodes treated with acid appears to be more significant. The higher improvement in current density can be seen from the lowest velocity to its double, which correspond to an average of 20%. Both electrodes present a linear dependence between the current density and the flow rate. The values of the resistance from Figure 2 are listed in Table 1:

The increase in the current density from the non-treated electrodes to the graphite felts treated with acid might be due to an increase in the electroac-

Table 1: Resistance values at different flow rate for the 0.15 M of V electrolytes with acid treated electrodes

Flow rate [mL/min]	R [$\Omega\text{-cm}^2$]
2.5	35.7
5	25
10	20
16	16

tive area of the electrodes due to the acid treatment. In fact, Figure 3 show some degradation on the carbon fibers. The maximum amount of current density recorded with the acid treated electrodes is 24 mA cm^{-2} at 0.95 V while for the non-treated electrodes is 8.5 mA cm^{-2} . The range of maximum output power for the acid treated electrodes is between 10 mW/cm^2 and 23 mW/cm^2 .

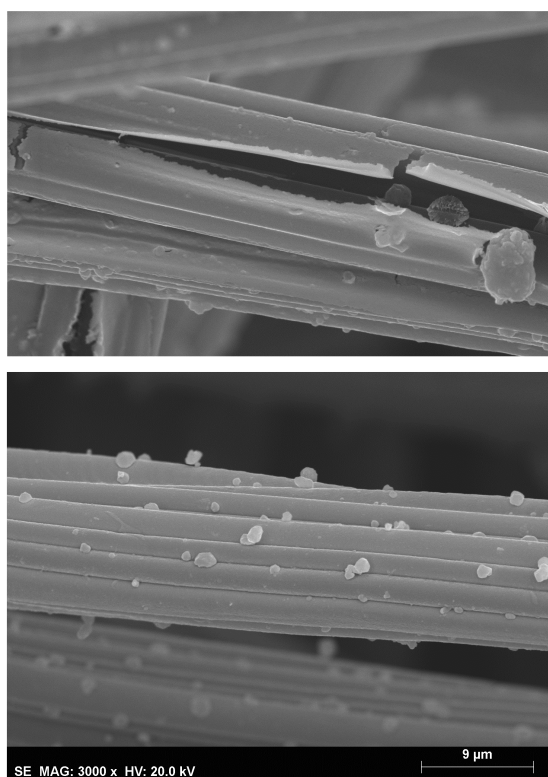


Figure 3: SEM images: non-treated electrode (top) and acid treated electrode (bottom)

4.4. Concentration influence on polarization behaviour

The solutions with the double of concentration were tested as well with the electrodes treated in acid, as they have shown in the past experiments a better performance. The values of the resistance from the polarization curves are reported in Table 2. The polarization plots for the solution of 0.3 M do not show the same characteristic trend as the polarization curves recorded so far. The activation losses are almost negligible. The more concentrated solutions do not show a dependence on the flow rate and it means there is no need to high turbulence in order to distribute

the solutions into the electrodes. Therefore, it is not convenient to work with high flow rates because of the power supplied to the pump. The tests are stable and does not modify its shape even presenting a long ohmic range. The increment of reagents in the electrolytes exhibits a remarkable enhancement on the performance of the battery, with current that results the double compared to the diluted solutions. While the 0.15 M solutions present a section where the concentration losses are evident in the 0.3 M solutions the losses do not appear relevant. The maximum value of current intensity recorded corresponds to 44 mA cm^{-2} . The value of the output power are not so different between the curves since the flow rate was not a key parameter. The range of output power is between 38 mW/cm^2 and 40 mW/cm^2 .

Table 2: Resistance values at different flow rate for 0.3 M of V solutions with acid treated electrodes

Flow rate [mL/min]	R [$\Omega\text{-cm}^2$]
2.5	10
5	10
10	9.7
16	9.4

4.5. Charge-discharge cycles

The results for four consecutive charge-discharge cycles for the non-treated electrode and the electrolytes of 0.15 M presented for each consecutive cycle the charge-discharge time is reduced by 2%. The reduction of the time of the cycle might be caused by the solution aging, which is correlated to the vanadium ion crossover through the membrane and the reaction associated to it or because of hydrogen evolution which is suppose to occur when the the potential overcome 1.6 V. Since the current efficiency of the system, according to the Equation 6, results to be higher than 90% for each cycle, the H_2 evolution is negligible. According to Equation 2.1 the working potential of the cell is between 1.3 V and 0.9 V. The evident drop in potential at the end of the discharge is caused by the mass transport effects that can be seen in some of the polarization curve in Figure 2. The use of the identical cell configuration with the double concentrated electrolytes suggests the time for each cycle will be doubled. From Figure 4 it is evident the time is increased of more than three times and a reduction in the cell internal resistance is evident. So the use of more concentrated solution enhance the performance of the battery.

There is an evident increment in the working potentials during the discharge and this is because the more concentrated is the solution the higher will be the voltage according to Equation 2.1. This affects the potential efficiency as well as the energy efficiency. According to Equations (6), (7) and (8) the average values for each modification are listed in Table 3. The acid treatment shows an improvement in the current efficiency

Table 3: Average value of current, potential and energy efficiency

	Current efficiency [%]	Potential efficiency [%]	Energy efficiency [%]
Non-treated electrodes 0.15 M of V	98.01	68.5	60.28
Acid treated electrodes 0.15 M of V	99.51	74.33	73.97
Acid treated electrodes 0.3 M of V	93.15	87.41	81.42

as well as in the potential efficiency and energy efficiency. The increase in the concentrations exhibits a decrease in current efficiency but an increase in voltage efficiency as expected and in the energy efficiency of the battery.

4.6. Concentration influence on the self-discharge

It could be expected that the membrane was more permeable to the solutions with more active species, but apparently the 0.3 M of V solutions took about fifteen times more time to self-discharge than the less concentrated electrolytes. The delay in self-discharging with the increase in concentration might be due to the difference in the viscosity of the solutions since the concentration was doubled for the vanadium as well as for the sulfuric acid. The difference in the trends is because the concentration affects the OCP and consequently the value for the 0.15 M electrolytes results lower.

4.7. EIS measurements

The Nyquist plots are characterized by two capacitive loops, plus an ohmic resistance corresponding to the high frequency interception of the real axis. The ohmic resistance is related to the electronic transport, the electrolytes and the resistance to ionic conduction. The semicircles characterize a resistance-capacitance behaviour, usually associated to the electrode/electrolyte double layer, the transfer of active species or the mass transport effects. The time constant were read from the Bode plots.

Under spontaneous conditions, steady state was not attained in the initial 45 minutes of discharge. The results that present the influence of the concentration on the EIS shows the low frequency capacitive loop has higher resistance for the curve with lower concentration. This is probably because of the presence of

more active species in the solutions leads to an increase in the current and consequently a decrease in the total resistance of the cell.

The effect of the membrane on the spectra was investigated by making an experiment in which two membrane were mounted in series. It was evident that the membrane contributes only to the ohmic resistance, it does not accumulate charge. The ohmic resistance went through a two-fold increase, which means that the resistance of the membrane is approximately 0.125Ω and since the area is 25 cm^2 the resistivity of the membrane will result to be $3.125 \Omega \text{ cm}^2$.

The spectra were analyzed using the equivalent circuit (EC) approach. The EC is build for the curve at different concentrations. The EC and the spectra with the respective fittings are shown in Figure 5.

Table 4: Value for the component of the EC

Element of the EC	Value	
	0.15 M of V	0.3 M of V
R0 [$\Omega \cdot \text{cm}^2$]	3.11	3.18
CPE1-Q0 [$\text{F} \cdot \text{s}^{n-1} / \text{cm}^2$]	0.0021	0.0010
CPE1-n	0.647	0.745
R1 [$\Omega \cdot \text{cm}^2$]	3.59	1.83
C2 [F / cm^2]	0.00153	0.0016
R2 [$\Omega \cdot \text{cm}^2$]	10.18	4.31

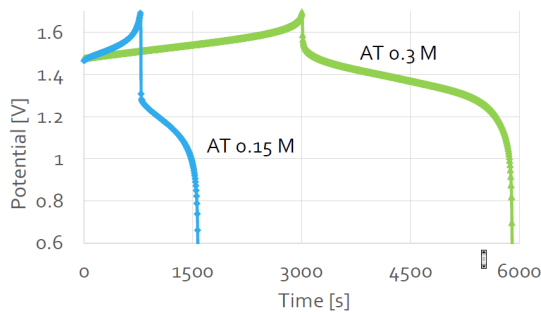
A time constant is associated to the equivalent circuit shown in Figure 5. The time constant is characteristic for a loop where a resistor and a capacitor are placed in parallel, in this case the equivalent circuit will be characterized by two time constants. It is defined as:

$$\tau = RC \quad (12)$$

Where R is the resistance and C the capacitance. Two time constant can be evaluated for each circuit. In particular for the more concentrated solution the time constant for the high frequencies, equivalent to the circuit with the CPE and the resistor is 0.001 s and the time constant for the low frequencies which comprises the resistor and the capacitor is 0.28 s. Concerning the solution less concentrated the time constants are 0.0025 s and 0.625 s for low and high frequencies respectively.

5. Discussion

The polarization behaviour of VRFB was broadly treated in literature. It was observed the scan rate influenced the polarization curve with a proportional increase of the current density with an increase in

**Figure 4:** Charge-discharge cycles with 0.15 M and 0.3 M of vanadium

the scan rate. This is confirmed by Hung et al. [14] that proves if the total variation of the polarization parameter in a period of time is the same, the frequency of increment had no effect on the polarization curves. Therefore, the main cause of the change in the electrochemical behaviour during polarization is due to the time to complete the polarization measurements. It causes significant reduction of redox active species in the electrolytes solutions. The results presented in literature about the dependence of the performance on the electrolyte flow rate have a similar behaviour obtained this work. The current increases proportionally to the volume flow rate until an optimal flow rate, after which it is not convenient because of the electric power supplied to the peristaltic pump. This may be due to the absence of specific flow geometry which may ensure a good recirculation of the electrolytes inside the reactor. In fact, the enhancement in the performance of VRFB with flow field has also been investigated by Xu et al. [15]. In particular, the flow field plays an important role to limit the mass transport effect at low potentials, allow the cell to provide 250 mA/cm^2 for 1 M vanadium concentration in 3 M sulfuric acid. Several carbon felt electrodes performance have been reported in literature. Although the non-treated electrode NATIONAL™ Carbon Felt grade VGD tested in this work had worked with low concentration of electrolytes, exhibited current density values between 150 and 250 mA/cm^2 . Nibel et al. [16] have tested non treated electrodes with more concentrated electrolytes presenting results comparable to what obtained in this work. The charge-discharge cycles tests presented current efficiency with higher value compared to the reported values, but for the potential efficiency and the energy efficiency the value results

to be lower [16]. The current intensity has increased of 40% compared to the non-treated electrodes. A higher increment is presented by Eifert et al. [17] on different graphite felt electrodes which is between 50% and 180%. This might be due to the degradation of the fiber shown in SEM images. Although it may have increased the active area, on the other hand the graphite felt might not have been resisted to the exposition to the aggressive environment for such long time. Regarding the charge-discharge cycles and the related efficiency the remarkable enhancement is on the potential efficiency which affects the energy efficiency as well. Sun and Skyllas-Kazacos [18] obtained value comparable with the efficiency values recorded in this work. In particular for the more concentrated solution, the carbon felt used in this work exhibited a higher potential efficiency and energy efficiency.

The reason behind the better performance is still debated. Zeng et al. [19] studied the increment of functional group units amount as performance improvement compared to the increase on the active area. The concentration of the electrolyte is crucial in the performance of the battery. The preparation of the electrolytes was carried out chemically. It was a simple and inexpensive method. The use of 0.3 M of vanadium which is just one third of the usual concentration used for energy storage showed good performance comparable with the literature. It may be because the electrode used has a large active area. Kim et al. [20] report tests on electrodes which have half of the thickness of the graphite felt used in this cell. The double amount of electroactive species had produced twice the current density and some times even three time more current density. Typical value of concentrations for operating VRFB

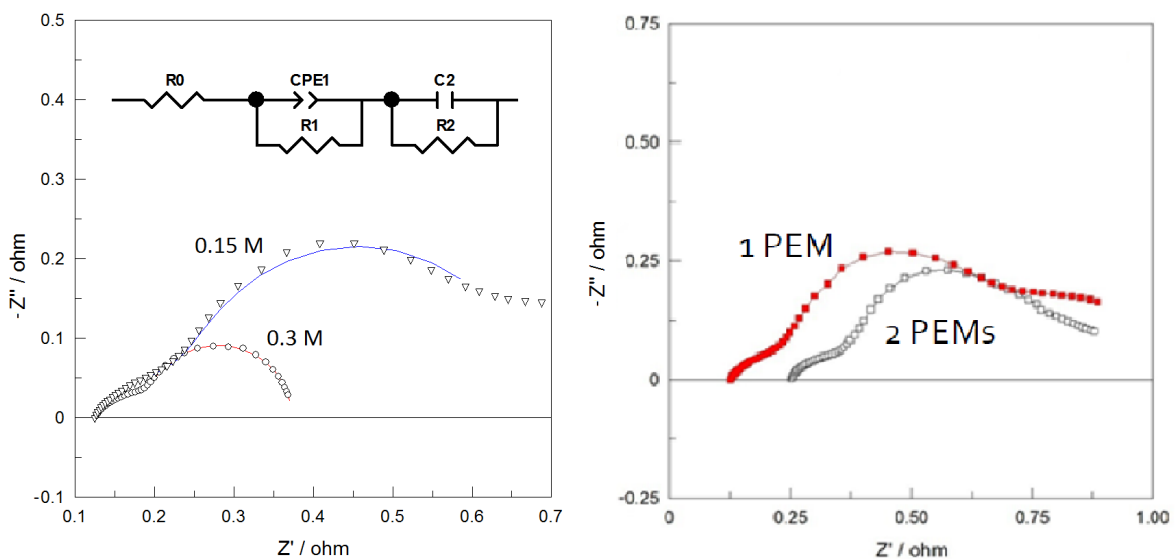


Figure 5: EC and fitting for 0.15 M solutions and 0.3 M solutions at 16 mL/min (left) and Nyquist plot for 1 membrane and 2 membranes in series (right)

are 1 M of vanadium in 2 or 3 M of sulfuric acid which lead to an increase in the potential of the cell according to Equation 2.1. Not only the vanadium ion concentration is important for the performance of the battery. The sulfuric acid concentration has a remarkable influence in the polarization curves, especially on the cell potential. In fact, according to Equation 2.1 the variation of the potential is about 120 mV/pH. Not only an increase in the voltage, Tsushima et al. [21] present an increase in the current density. In particular from 1 M to 4 M of H_2SO_4 concentration the current density increases from 85 mA/cm^2 to 200 mA/cm^2 for the same electrochemical cell configuration. With respect to the self-discharge behaviour, several studies have been presented aiming to understand the reagent crossover through the membrane, the main causes of self-discharge and contamination of the solutions. The outcome obtained in this work show a dependence of the self-discharge on the concentration of the reagents and the solvent. The more concentrated the solution is, more time will be necessary to register a drop in the potential due to vanadium ions crossover or water transport through the membrane. The result meets what has been reported in literature. Lawton et al. [22] show a dependence on concentration of the solvent and the solute. It affects the viscosity of the electrolytes making the crossover more difficult. In particular, doubling the concentration of sulfuric acid will increase by 50% the viscosity of the solutions [23]. To our knowledge the space-time characteristic of these cell has not been reported in literature. This is however an important parameter. It is deeply correlated with the fluid dynamics of the electrolyte inside the cell and it can be used to determine easily the conversion rate and to help define the optimal working conditions and an immediate way to understand how long the solution will remain inside the electrochemical reactor. It is also relevant to understand the mass effects inside the cell, especially when there is no flow geometry. From the Figure 1 some species are fast converted while some other take a longer path to come out probably because of stagnation points. The conversion efficiency has room to improvements. The time evolution of the EIS tests shows an increment in the internal resistance of the cell which meets the results obtained by Jeong et al. [24]. The impedance spectra present a higher resistance when it comes to the solution with 0.15 M of V compared to the 0.3 M of V which meet the results obtained in the DC polarization curves. The membrane had shown a purely resistive behaviour during AC polarizations and the same outcome is obtained by Zago and Casalegno [25]. The EIS shows two capacitive loops, one at high frequencies and one at low frequencies respectively. The low frequency capacitive loop is assigned to the concentration

influence, since it becomes smaller when the solution with the double of concentration is tested. It may be due to the electrode double layer of the transfer of the active species. The high frequency capacitive loop might be related to the contact resistance between the current collectors but further tests are needed in order to confirm this theory. Zago and Casalegno [25] shows two capacitive loops as well. With a mathematical model it relates the high frequency capacitive loop to the charge transfer phenomenon while the low frequency capacitive loop is due to diffusion and convection. In Nyquist plot the diffusion phenomenon appears to be a straight line which goes up to infinite and in the Bode plot as linear relationship between $\log(|Z|)$ versus $\log(\theta)$ with a slope value of 45 degrees, represented on the equivalent circuit as Warburg element and it is not present either in this work or in [25]. The EC resistance for the two different solutions presented in Table 4 correspond to the same value obtained from the polarization curves in DC at 16 mL/min flow rate listed in Table 1 and Table 2. To our knowledge, most of the studies about EIS on VRFB have been conducted usually just in half-cell and consists of just one capacitive loop [26, 27, 28].

6. Conclusions

The vanadium redox flow battery was handmade from the raw material. The best performance were obtained through the use of the acid treated electrode, the solution of 0.3 M and the maximum flow rate of 16 mL/min.

Although the treatment with sulfuric acid presented some degradation on the carbon felt it exhibited improvement on the performance of the cell. The low concentration due to solubility constraint of the vanadium raw material was not a barrier because the output current densities obtained were comparable with the literature. The influence of the flow rate was found not relevant in solution with more concentration of active species. In particular the cell in its best configuration was characterized by a potential working range between 1.6 V and 1.2 V, a maximum output power of 40 mW/cm^2 and a energy efficiency of 81.4%.

It was possible to describe the electrochemical behaviour of the cell with an equivalent circuit. In particular it has been proven the pure resistive behaviour of the membrane.

At last, the objectives established at the beginning where all achieved, developing a small scale VRFB for energy storage with lower costs, although more tests would have needed to be performed in order to better understand the mechanisms that occur into the electrochemical cell.

References

- [1] W. Wang, L. Qingtao, B. Li, X. Wei, L. Li, and Z. Yang. Recent progress in redox flow battery

- research and development. *Adv. Funct. Mater.*, 2012.
- [2] L. H. Thaller. US-Patent 3 996 064, 1976.
- [3] Dong-Jun Park, Kwang-Sun Jeon, Cheol-Hwi Ryu, and Gab-Jin Hwang. Performance of the all-vanadium redox flow battery stack. *J. Ind. Eng. Chem.*, 45:387–390, 2017.
- [4] David Reed, Edwin Thomsen, Bin Li, Wei Wang, Zimin Nie, Brian Koeppel, and Vincent Sprenkle. Performance of a low cost interdigitated flow design on a 1 kw class all vanadium mixed acid redox flow battery. *J. Power Sources*, 306:24–31, 2016.
- [5] Zhijiang Tang, Douglas S. Aaron, Alexander B. Papandrew, and Thomas A. Zawodzinski Jr. Monitoring the state of charge of operating vanadium redox flow batteries. *ECS Transactions*, 41:1–9, 2012.
- [6] C. A. Vincent and B. Scrosati. *Modern batteries - An introduction to electrochemical power sources*. Butterworth-Heinemann, 2nd edition, 1997.
- [7] C. Blanc and A. Rufer. Understanding the vanadium redox flow batteries. In book: Path to sustainable energy, Nov 2010.
- [8] D. Aaron, Z. Tang, A. B. Papandrew, and T. A. Zawodzinski. Polarization curve analysis of all-vanadium redox flow batteries. *J. Appl. Electrochem.*, 41:1175–1182, 2011.
- [9] E. Agar, C. R. Dennison, K. W. Knehr, and E. C. Kumbur. Identification of performance limiting electrode using asymmetric cell configuration in vanadium redox flow batteries. *J. Power Sources*, 225:89–94, 2013.
- [10] C. Sun, F.M. Delnick, L. Baggetto, G.M. Veith, and T.A. Zawodzinski Jr. Hydrogen evolution at the negative electrode of the all-vanadium redox flow batteries. *J. Power Sources*, 248:560–564, 2014.
- [11] H. Liu, Q. Xu, C. Yan, and Y. Qiao. Corrosion behavior of a positive graphite electrode in vanadium redox flow battery. *Electrochim. Acta*, 56: 8783–8790, 2011.
- [12] X.G. Yang, Q. Ye, P. Cheng, and T.S. Zhao. Effects of the electric field on ion crossover in vanadium redox flow batteries. *Appl. Energy*, 145:306–319, 2015.
- [13] Andrzej Lasia. *Electrochemical Impedance Spectroscopy and its Applications*. Springer, 2014.
- [14] Y. Hung, Y. Bu, J. Kubin, and D. Weinman. Effects of current scan rate on the polarization curve of vanadium redox flow batteries. *International Energy and Sustainability Conference (IESC)*, 2017.
- [15] Q. Xu, T.S. Zhao, and C. Zhang. Performance of a vanadium redox flow battery with and without flow field. *Electrochim. Acta*, 142:61–67, 2014.
- [16] O. Nibel, S. Taylor, S.M. Patru, A. Fabbri, E. Gubler, and T.J. Schmidt. Performance of different carbon electrode materials: Insights into stability and degradation under real vanadium redox flow battery operating conditions. *J. Electrochem. Soc.*, 164(7):A1608–A1615, 2017.
- [17] L. Eifert, R. Banerjee, Z. Jusys, and R. Zeis. Characterization of carbon felt electrodes for vanadium redox flow batteries: Impact of treatment methods. *J. Electrochem. Soc.*, 165(11): A2577–A2586, 2018.
- [18] B. Sun and M. Skyllas-Kazacos. Chemical modification of graphite electrode materials for vanadium redox flow battery application - part ii. acid treatments. *Electrochim. Acta*, 13:2459–2465, 1992.
- [19] L. Zeng, T. Zhao, and L. Wei. Revealing the performance enhancement of oxygenated carbonaceous materials for vanadium redox flow batteries: Functional groups or specific surface area? *Advanced sustainable systems*, 2(2), 2017.
- [20] K. Kim, M. Park, Y. Kim, J. Kim, S. Xue Dou, and M. Skyllas-Kazacos. A technology review of electrodes and reaction mechanisms in vanadium redox flow batteries. *J. Mater. Chem. A*, 33, 2015.
- [21] S. Tsushima, S. Sasaki, and S. Hirai. Influence of cell geometry and operating parameters on performance of a redox flow battery with serpentine and interdigitated flow fields. *ECS, Meeting abstracts*:1164, 2013.
- [22] J.S. Lawton, A. Jones, and T. Zawodzinski. Concentration dependence of VO_2^+ crossover of nafion for vanadium redox flow batteries. *J. Electrochem. Soc.*, 160(4):A697–A702, 2013.
- [23] F. H. Rhodes and C. B. Barbour. The viscosities of mixtures of sulfuric acid and water. *Ind. Eng. Chem.*, 15:850–852, 1923.
- [24] S. Jeong, L.H. Kim, Y. Kwon, and S. Kim. Effect of nafion membrane thickness on performance of vanadium redox flow battery. *Korean J. Chem. Eng.*, 31(11):2081–2087, 2014.
- [25] M. Zago and A. Casalegno. Physically-based impedance modeling of the negative electrode in

all-vanadium redox flow batteries: insight into mass transport issues. *Electrochim. Acta*, 248: 505–517, 2017.

- [26] C. Sun, F.M. Delnick, D.S Aaron, A.B. Papan-drew, M.M. Mench, and T.A. Zawodzinski. Resolving losses at the negative electrode in all-vanadium redox flow batteries using electrochemical impedance spectroscopy. *J. Electrochem. Soc.*, 161:A981–A988, 2014.
- [27] J. Noack and J. Tubke. A comparison of materials and treatment of materials for vanadium redox flow battery. *ECS Transactions*, 25(35), 2010.
- [28] I. Derr, M. Bruns, J. Lagner, A. Fetyan, J. Melke, and C. Roth. Degradation of all-vanadium redox flow batteries (vrfb) investigated by electrochemical impedance and x-ray photoelectron spectroscopy: Part 2 electrochemical degradation. *J. Power Sources*, 325:351–359, 2016.